X-912-76-133
PREPRINT

ION COMPOSITION IN A NOCTILUCENT CLOUD

R. A. GOLDBERG

G. WITT

JULY 1976

GSFC

GODDARD SPACE FLIGHT CENTER
GREENBELT, MARYLAND

X-912-76-133
Preprint

ION COMPOSITION IN A NOCTILUCENT CLOUD

R. A. Goldberg

(Atmospheric and Hydrospheric Applications Division)

G. Witt

(Institute of Meteorology, University

of Stockholm, Stockholm, Sweden)

July, 1976

GODDARD SPACE FLIGHT CENTER

Greenbelt, Maryland

ION COMPOSITION IN A NOCTILUCENT CLOUD

R. A. Goldberg

(Atmospheric and Hydrospheric Applications Division
NASA/Goddard Space Flight Center, Greenbelt, Maryland 20771)

G. Witt

(Institute of Meteorology, University
of Stockholm, Stockholm, Sweden)

ABSTRACT

Ion composition at mesospheric altitudes has been measured and compared between high and mid-latitude sites under summer daytime conditions. Both rocket-borne measurements were made with pumped quadrupole ion mass spectrometers (mass range: 15 → 145 AMU). Apogee occurred below 90 km on each flight permitting subsonic sampling near the mesopause. Water cluster dissociation was further minimized by using low attractive bias potentials of -5V for each instrument. The mid-latitude data were obtained at Wallops Island, Virginia (latitude = 37.8°N; longitude = 75.5°W) on June 30, 1973 at 1510 LMT (χ = 43°). Here, large quantities of hydronium cluster ions were observed through 109^+, with maximum concentrations at 55^+ and 73^+. Also, cluster ions of nitric oxide were observed through 84^+. The high latitude launch occurred at Kiruna, Sweden (latitude = 67.9°N; longitude = 21.1°E) on August 2, 1973, at 0700 LMT (χ = 68.5°) following visual sighting of a noctilucent cloud on the prior evening. The data near mesopause shows the typical cluster ions mentioned

above, but also a preponderance of heavy ions between 90 and 145 AMU, with groupings 18 AMU apart but unrelated to the more typical cluster ions. One possible set of consistent identifications leads to iron and iron oxide hydrates. These results may suggest the presence of metallic particulates and ions which form hydrated clusters ions within the cloud region.

CONTENTS

TABLES

FIGURES

FIGURES (Con\ )

FIGURES (Continued)

ION COMPOSITION IN A NOCTILUCENT CLOUD

INTRODUCTION

Noctilucent clouds (NLC) occur at altitudes near the mesopause (~85 km) and are the highest cloud formation known to exist in the Earth's upper atmosphere. Visual sighting of these clouds is primarily restricted to high latitudes for a three month period in Summer, and can only occur near twilight when viewing conditions are optimum (e.g., numerous papers on NLC behavior in Proceedings of International Symposium on NLC, 1967). This period also provides an extremely cold and well defined temperature minimum at the mesopause (Theon et al, 1967), which is believed to be a significant requirement for NLC formation. Recent satellite evidence (Donahue et al., 1972) has indicated that NLC displays exist at high latitudes on a nearly permanent basis during summer, which might imply that the highly erratic sightings from ground and aircraft are at least in part a manifestation of variability in viewing conditions and brightness contrast, as well as cloud presence.

Interest in NLC has been sustained and advanced for more than 75 years, since the discovery of their mesospheric location by triangulation techniques (Jesse, 1896). At present, no unique determination of the cloud composition nor of processes for NLC formation have been established. These questions are important from mesospheric considerations, and because of the possible information the answers might provide concerning stratospheric aerosol formation

from the gas phase. Study of NLC in this context may thereby be useful in the investigation of solar-climatic control through aerosol formation in the upper atmosphere (Hummel and Olivero, 1976).

Most proposed mechanisms for NLC formation require the presence of water vapor (Witt, 1969; Reid, 1975), and/or extraterrestrial materials (Witt, 1969, Fiocco and Grams, 1971). Furthermore, molecular and atomic species in an ionized state are most likely to provide nuclei for sublimation and other nucleation processes (Castleman, 1974). The experiment reported here was predicated upon these assumptions, and the results to be shown exhibit evidence for the validity of a metalic ion/water nucleation process. In this work, we report and analyze two rocket-borne studies of ion composition at mesospheric altitudes with mass spectrometer techniques. This study represents a comparison of mid- (Wallops Island, Va.) and high-latitude (Kiruna, Sweden) summertime results under nearly identical instrumental sampling conditions. The data from high latitude are thought to contain ionic structure within a NLC, and show significantly different structure than those normally obtained at high latitudes in both summer (Johannessen and Krankowsky, 1972) and non-summer periods (Zbinden et al., 1975) and at other latitudes during all periods (e.g., Narcisi and Bailey, 1965; Goldberg and Aikin, 1971).

PAYLOAD AND LAUNCH CHARACTERISTICS

NASA 10.412 and 10.414 specify Nike Cajun launches of two ion mass spectrometer payloads in the summer of 1973. The first was from Wallops

Island, Va. (37.8 N, 75.5 W; I (magnetic dip) = 68.8°) and the second from Kiruna, Sweden (67.9°N, 21.1°E; I = 76.7°). The characteristics of each launch are described in Table 1.

Each of the above identical payloads consisted of a quadrupole ion mass spectrometer (Goldberg and Blumle, 1970; Goldberg and Aikin, 1971) to measure ion composition, a Gerdien probe to determine total ion density (Aikin et al., 1972) and Faraday rotation radio propagation experiments at both 3.030 and 6.9825 MHz (e.g., Aikin et al., 1964) for electron density. Additional magnetometers and solar sensors were employed for payload aspect.

The characteristics of each mass spectrometer are featured in Table 2. In an attempt to search for heavy cluster ions, each instrument was designed to sweep to masses above 145 AMU. The earlier results of Narcisi and Roth (1970) and Goldberg and Aikin (1971) have demonstrated probable dissociation of heavy water cluster ions within the high pressure field behind the ram shock, causing modification of the ambient distribution prior to sampling. Furthermore, Goldberg and Aikin (1972) demonstrated that an attractive bias potential in excess of -10 volts and applied at the spectrometer sampling orifice could severely modify the incoming distribution. These problems were minimized by use of -5 volt attractive bias potentials and through the following flight procedures.

Each payload was separated from the rocket motor at 60 km on upleg. This minimized contamination from outgassing of the rocket motor and also

provided a spin stabilized platform to altitudes below 70 km on downleg. The latter feature permitted wake sampling to low altitudes, as recommended from our earlier findings (Goldberg and Aikin, 1971). Each payload carried additional ballast to reduce apogee to below 90 km, thereby allowing sampling to occur near the mesopause under subsonic conditions. These features are illustrated in Figure 1, where comparison of a trajectory with apogee near 80 km is made with our more standard payload trajectory near 125 km. Conditions of ram or wake sampling are defined for $\alpha < 90°$ or $\alpha > 90°$ respectively. This technique also provided improved height resolution for the data near the mesopause, which was a desirable feature to counteract the reduced height resolution induced by the lengthy sweep range of the spectrometers.

Finally, the spectrometer aboard 10.414 was adjusted for increased sensitivity at the expense of mass resolution. This adjustment was made to compensate for reduced ambient ion densities, which were expected to occur under the large solar zenith angle conditions required for early morning sampling at high latitude. This prevented unique identification of mass values above 50 AMU, but did permit the detection of heavy mass ions in excess of 110 AMU.

DATA ANALYSIS

The Wallops Island flight on June 30 was designed to provide optimum data sampling under controlled conditions, for a typical mid-latitude daytime summer mesosphere during quiet solar conditions. The flight in Kiruna on August 2 was then made to compare the high latitude daytime summer mesosphere under

nearly identical conditions. Visual sighting of a strong NLC display near the predicted downrange apogee location of the rocket flight was made from an aircraft near midnight on the evening of August 1. Rocket launch was delayed until the following morning when an adequate D region would exist for positive ion sampling. Regrettably, no independent measurement of NLC presence could be made during the launch period. The continued presence of the NLC during the data acquisition period was assumed on the basis of the conclusions discussed earlier, and appears verified by the unusual results reported here.

Figure 2 illustrates a sample raw data spectrum obtained near apogee from the Wallops Island control shot. The data are presented on a quasi-logarithmic scale (each volt above one (1) volt represents approximately one decade in sensitivity). The AC voltage sweep is also presented to demonstrate the linearity of the sweep. The double flat topped peaks preceding and following the ramp portion of the sweep relate to high pass filter mode data, and are not pertinent to the discussions in this work. Finally, the data show a slow response recovery at the base level following each spectral peak. This behavior was attributed to an electrometer malfunction rather than an external background source (e.g., photons or particles), and was treated as a non-additive background component during the subsequent data analysis.

Figure 3 shows similar spectral data for the high latitude flight at Kiruna. In this case, the full sequence of spectra obtained from 87 to 73 km on downleg is shown to illustrate the sudden appearance and disappearance of heavy ion groups within the NLC regime. The running altitude of the data sample is displayed

on the abscissa. The designation 10.414A represents one possible interpretation of mass peak identification. Here, the arrow markers denote location for the specified mass, but do not necessarily refer to the observed peaks. Hence, 148^{+} simply specifies the maximum mass limit for this identification grouping.

The data have also been subjected to a rescaling in which the peak mass limit is shifted 2 AMU downward to 146^{+}. This scaling (10.414B) appears to provide results which are more consistent in the mass range above 70 AMU, e.g., it identifies the heavy mass peak near 84 km as 127^{+}, which could be an oxonium water cluster ion. It also represents the lowest value which will not disturb the more established peak identifications at low mass. Hence, the "B" identifications are used to produce the profile presentations shown later in this work. Consistency arguments based on positive identification of light mass peaks (19^{+}, 30^{+}, 32^{+}) imply error limits of ±2 AMU near 150 AMU, ±1 AMU near 100 AMU, and ±1/2 AMU below 50 AMU. However, such ranges in mass identification do not seriously alter the results of this work concerning heavy ion structure within an NLC.

Because of cluster ion dissociations under ram sampling conditions, only downleg data are considered here. These data are presented as vertical profiles in Figures 4 (10.412) and 5 through 7 (10.414B). The curve labelled N_i refers to the absolute total ion density, obtained from a combined analysis of the Faraday and Gerdien data during the upleg portion of the flight. Above 70 km, negative ions were assumed absent, so that the total electron density

profile (Faraday data) can be equated to N_i. Below 75 km, the Gerdien ion density was superimposed producing the low altitude portion of the N_i profile (to 65 km) on each flight.

Absolute magnitudes of each ion species were obtained by normalization of the measured spectral currents to the total ion density value (N_i) at the mean height for each spectrum. No mass weighting was applied in the normalization procedure, since all data were obtained at low velocity at altitudes below the free molecular flow regime. Effects induced by reduced instrument sensitivity with increasing mass have also been neglected in this analysis. Hence, it must be assumed that the magnitudes for the heavier masses are lower bounds, and could be enlarged if strong mass weighting effects exist and must be corrected for, especially in the transition flow region from 90 to 65 km.

RESULTS

A. Spectra

The flight at Wallops Island (10.412) was designed to obtain a typical mid-summer profile of daytime mesospheric ion composition. The sample spectrum displayed in Figure 2 was obtained during the downleg portion of the flight near 86 km. These data exhibit the established ionic species (30^+, NO^+; 32^+, O_2^+) including the oxonium and nitric oxide cluster chains, i.e., $H_3O^+ \cdot (H_2O)_n$ and $NO^+ \cdot (H_2O)_m$. In this figure, the maximum values of n and m are 4 and 3 (91^+ and 84^+), respectively. During upleg between 85 and 86.5 km, n = 5 (109^+) was also observed briefly (Figure 4). The mass 64^+ ($O_2^+ \cdot O_2$ or $NO_2^+ \cdot H_2O$)

is also in evidence as a small peak to the left of 66^+. This is the first appearance of 66^+, 84^+ and 109^+ in our mid- and low latitude data, and is attributed to the improved sampling procedures involved in this flight. Finally, H_30^+ (19^+) is conspicuous by its absence, and only appeared in spectra obtained during upleg supersonic ram conditions. This seems to verify an earlier result (Goldberg and Aikin, 1972) that 19^+ in the mesosphere may normally be regarded as a dissociation product caused by sampling procedures.

Figure 3 illustrates the downleg data obtained between 87 and 73 km aboard 10.414 in Kiruna. The resolution here, although inferior, is adequate to establish multiple peaks within the groupings labelled A→E. These groupings are meant to infer multiple mass structure about each of the hydronium cluster ions 55^+, 73^+, 91^+, 109^+ and 127^+. Although each grouping is spaced approximately 18 AMU apart, the extreme mass range limits within the group do not match this spacing between groups. We are confident that multiple mass peaks exist within each group because of the reasonable resolution at high mass for the two peaks near 80 km, and by the multiple ridges observed near the top of each major group elsewhere.

The most striking feature of these spectra is the dramatic appearance of groups C, D and E between 86 and 82 km. This is correlated with an increased width of groups A, B, 37^+ and 48^+ within this region, and by the sudden disappearance of masses 19^+, 64^+ and 66^+ below 82 km. The increased spectral structure at high mass near 86 km also appears real since it disappears at

lower altitudes in both ram and wake sampled spectra. This high mass structure could represent less common hydrated and non-hydrated molecules formed by extraterrestrial matter. The features of this region are quite unique and have not been reported for other high latitude mass spectrometer measurements during summer (Johannessen et al., 1972; Johannessen and Krankowsky, 1972) or winter (Zbinden et al., 1975) conditions. The heavy ion structure above the cloud region also appears to correlate with an enhanced total ion density near 88 km (cf. section B below) in concurrence with earlier independent observations of Pedersen and Derblom (private communications) during an August 10, 1970 NLC display. These comparisons, plus the sighting of a NLC on the night prior to launch, are offered as evidence that the observed data shown here include ionic structure within the NLC cloud region.

B. Composition Profiles

Figure 4 compares the normalized vertical composition for NASA 10.412 obtained during upleg and downleg portions of the flight. N_i represents the independently measured total ion density profile used as the normalization reference. The figures designate each constituent with a most probable molecular identification, based on widely discussed aeronomic considerations in the literature. The upleg data are presented to illustrate the similarity with downleg data when ram sampling is conducted under subsonic conditions (within four kilometers of apogee). Below 83 km, most cluster ions show higher abundances in the downleg portion of the flight. Excepted are 19^+ and 37^+, which show

more abundance below 80 km on upleg, suggesting these species to be (in part) dissociation products of heavier cluster ions subjected to supersonic ram sampling conditions. Below 80 km on downleg, there is also an increased absence of heavy cluster ions, which may be partially caused by supersonic wake sampling conditions. However, no reoccurence of 19^+ is observed in this region. Finally, traces of Fe^+ (~ 10 cm^{-3}) were observed near apogee but are not included on the figure.

Figures 5, 6 and 7 illustrate the downleg normalized ion concentration profiles for the Kiruna (10.414) flight using "B" identifications. Because of the large number of species identified in these data, the profiles are divided into three overlapping groups (one per figure) by mass number, i.e. $19^+ \rightarrow 55^+$, $55^+ \rightarrow 74^+$, $73^+ \rightarrow 141^+$. In each case 30^+ and 32^+ are repeated for cross reference. No molecular identifications are provided since the 10.412 identifications hold for the same mass ions here. Furthermore, many of the other less common species can have a multiplicity of identifications which are subject to a correct interpretation of the aeronomy involved, as well as to the previously discussed inaccuracies caused by reduced mass resolution. In some cases, two mass number identifications might represent the same mass (e.g., 54^+ and 55^+ in Figure 5), which could cause readjustment of the normalized values if this be the case. The separate identifications for 36^+ and 37^+, 54^+ and 55^+, $71^+ \rightarrow 74^+$, etc. are thought to be real under the criteria established for "B" scaling. No ion cluster upleg data are presented since they contain ram sampling modifications similar to those discussed for the data of 10.412.

Figure 8 presents the metallic ion profiles observed on 10.414. In this case, upleg data are presented because a) higher sensitivities are obtained for these trace species under ram sampling conditions and b) no modification of atomic ions through ram sampling is possible. The cluster ion 55^+ is included to demonstrate where Fe^+ (56^+) is thought to occur and be contained within the Group A peak (i.e., above 86 km). This is consistent with the appearance of other more easily identified metallic species (e.g., Mg^+; 24^+) within the same region.

A comparison of the total density (N_i) profiles between Wallops Island and Kiruna shows a dramatic enhancement for Kiruna, approaching a factor of 10 both above 85 km and below 70 km. This enhancement occurs in spite of the significantly larger solar zenith angle (χ) during acquisition of the Kiruna data. This result suggests an additional ion production source caused by precipitating electrons during the Kiruna measurement, although magnetic conditions were not unusually disturbed ($A_p = 16$). At the higher altitudes (near and above 85 km), direct ionization by energetic electrons would occur, while below 75 km, enhanced ionization induced from X-ray bremsstrahlung radiation would be possible. This interpretation is consistent with the composition data, which show a higher ratio for $32^+/30^+$ at Kiruna, as one would expect from an increased O_2^+ production through corpuscular ionization processes. The presence of the 19^+ in the low velocity wake data of this flight (where dissociation effects should be minimal) is further evidence for particle ionization at this time, since H_3O^+ is thought to be

produced solely by the O_2^+ hydration mechanism. We also note that the largest N_i enhancement occurs within and just above the NLC region, and can be attributed to those species which uniquely contribute to the high mass groups A, B, C, D, and E only within this altitude domain. A consistent set of mass identifications has been established for those mass peaks, and will be discussed in the following section.

DISCUSSION

Modern theories concerning NLC formation favor a structure composed of water particulates, formed near the mesopause by water collection on some type of nucleating agent. Basic ingredients for these theories require a sufficiently cold and wide mesopause, a source of molecules or particulates above the mesopause to act as nucleating agents, and sufficient water vapor to supersaturate the environment and permit nucleation to occur. In some cases, an upward motion is also required to permit particle growth to the observed macroscopic size. The water-nucleation theory is desirable in order to describe the continuously changing panorama of NLC. Furthermore, it is the only known mechanism capable of explaining the distinct lower boundary of the cloud layer (Witt, 1969).

Variability of NLC on a local scale was first demonstrated through ground observations of wave structure within the clouds (e.g., Störmer, 1933; Grishin, 1961; Witt, 1962). Recently, significant variability in thickness and height has also been established from rocket-borne photometric studies (Witt

et al., 1974). The satellite results of Donahue et al., (1972) define a spatially broad layer near the mesopause during summer, covering most of the northern polar cap in a quasi-permanent fashion. These observations do not describe the structure in sufficient detail to establish whether or not patches suitable for ground observation might be imbedded in an otherwise invisible layer. Furthermore, the results imply decreasing regularity in the layer structure with decreasing latitude leading to a minimum viewing period between 50-60° latitude near midsummer. Finally, as discussed earlier, some irregularities in ground based sightings may be caused by variability in suitable viewing conditions. However, NLC are observed up to several consecutive days during the appropriate viewing period for a specific site. Day to day modulations in the NLC structure observed in this manner probably represent dynamical changes in NLC behavior, rather than perturbations caused by viewing constraints.

At this time, only one of the three ingredients required for NLC theory has been demonstrated. The presence of a cold mesopause in summer was measured by Theon et al. (1967), and Witt (1967) has used this limited data to compare NLC presence with the coldest profiles. The problem of sufficient water vapor for supersaturation of the mesopause is more acute. Christie (1969a) and Witt (1969) both stressed the need for dynamic lifting of water vapor to produce supersaturation. Hesstvedt (1969) estimated that upward flux velocities of 10-20 cm/s were needed to produce the minimum size particulates of 0.1μ required for a visible cloud. The theory proposed by Christie (1969b), that gravity wave induced turbulence could be the upward driving force, was suggested from correlations

between the polar jet stream and NLC sightings, a correlation which has not been verified by further analysis. A possible solution has recently been offered by Reid (1975), who suggests that non-spherical crystal growth in this region need not require such large quantities of water vapor for production of visible size particles. This may be a possible answer, but must remain a hypothesis because of the unknown physical growth processes for water particulates at the mesopause.

Particulate size has been determined from the polarization and color of the scattered cloud radiance. For example, rocket-borne measurements at 68°N latitude (Witt, 1969; Tozer and Beeson, 1974) imply a 0.1 to 0.2 μ maximum radius, which is in agreement with the estimated size from OGO 6 data (Donahue et al., 1972; Hummel and Olivero, 1976). Gadsden (1975) on the other hand, has used ground based polarimeter techniques to estimate particulate sizes three times larger, and further claims non-spherical particulate shapes, as evidenced by the observation of eliptically polarized scattered light. Gadsden's result has not been confirmed by independent techniques, but if correct would help verify Reid's hypothesis.

Although direct experimental evidence for supersaturated water within and above NLC's is lacking, this requirement still remains as the only viable mechanism for explaining NLC formation. A comparison of Figures 5, 6, and 7 with Figure 3 shows that within the NLC region of the Kiruna flight, there are strong enhancements of the heavy oxonium cluster ions 73^+, 91^+, 109^+, and 127^+ when

compared to the more typical data of Wallops Island. (In Figures 6 and 7, 73^+ and 74^+ should be considered identical and overlapping for the purpose of this discussion.) Above 85 km, we also find much larger quantities of 66^+ and 64^+ in the Kiruna data. These species are observed to track 48^+ and 46^+, and are thereby identified as $NO^+ \cdot (H_2O)_2$ and $NO_2^+ \cdot H_2O$, respectively. The enhancement of the above hydrated species plus the appearance of other species in Groups B-E, which represent hydrates not normally seen (see below) may imply an increased abundance of H_2O in this region.

Attempts to measure and identify the nucleating agents as dust particles (e.g., Hemenway et al., 1964) have not provided positive identification nor reproducible results. These have led Soberman (1969) to suggest that submicron particles of zodiacal dust, rather than meteoric dust, might be the responsible agent. On the other hand, Fiocco and Grams (1971) have employed the diffusion transport-theory of Chapman and Kendall (1965) to argue that the estimated quantities of meteoric dust entering the earth's atmosphere each year are consistent with quantities needed to cause NLC. No account of water evaporation off dust particle surfaces caused by radiative heating is considered in their analysis, although such effects could prevent sublimation from occurring.

Witt (1969) has suggested that nucleating agents might be water clusters about metallic or molecular ions, and Hesstvedt (1969) also suggested Fe^+ as a most probable source. The data discussed in this analysis can be identified to provide a consistency argument for these suggestions. Using 10.414B identifications, the groups A→E are used to provide the identifications shown in

Table 3. Except for the oxonium series, all species relate to Fe^+, its oxides and hydrates. These identifications are satisfying in that they explain why the first and last mass of each group are not necessarily 18 AMU apart from those of adjoining groups. Fe_2^+ is provided as questionable, since it is difficult to produce this ion because of weak bonding; yet other identifications using 112^+ or 113^+ do not provide hydrated, oxide or any other form of ion starting with a reasonable atmospheric base constituent. Most species in the table are observed at least once, with the possible exception of 106^+ and 124^+. Finally, we note that all species identified show a maximum value in the NLC region.

The presence of Fe^+ at altitudes between 85 and 90 km is not unreasonable, and can be attributed to disintegration of meteoric matter. Most meteoric showers deposit meteoric material between 85 and 100 km, causing a world-wide metallic ion peak near 93 km. When the incoming material is of higher density or reduced velocity, ablation occurs at lower altitudes, as is the case for the ι Aquarids shower which was predicted to be in progress for the two-week period preceding the measurement (Millman and McKinley, 1963). A view of the upleg data of 10.414 (Figure 8) does show the appearance of Fe^+ ions above 85 km, which is consistent with the above description. We note that Mg^+ is less than Fe^+ by a factor of 5, implying the entry of material excessively rich in iron below 90 km (normally Fe^+ and Mg^+ are of the same magnitude). Finally Castleman (1974, 1976), has pointed out from laboratory results that Fe^+ is indeed a favorable metallic ion species for nucleation. These observations may explain in part, why hydrated and other compounds of Mg^+ cannot be identified.

Further indication for the presence of extraterrestrial matter in the 85 to 90 km is reported by Rauser and Fechtig (1972). Using an in situ sampling detector, they report maximum "dust" collection during an NLC display near 87 km, on August 10, 1970 during the Perseids meteor shower which, coincidently, overlaps the peak period of the ι Aquarids shower. The numerous atomic and molecular species caused by the ablation of and in residence with such matter could be responsible for the observed structure at high mass in the spectra obtained above 85 km. Also, later during the same display, one of us (G. W.) was able to deduce the presence of an excessive abundance of large particulates between 90-120 km, by measuring the unpolarized component of scattered light with rocket-borne photometers. This suggests the presence of a descending cloud of meteoric debris as an additional source of low altitude material, but not necessarily of atomic ions.

The data presented here thereby appear consistent with the theories which require the uplifting of water vapor to a supersaturated concentration within and above the cold summertime mesopause. This water vapor then forms complexes with Fe^+ and other ions, leading to stable condensation nuclei which subsequently grow and gravitationally descend as NLC particles. Recently, evidence that large hydrated clusters can be formed in low temperature conditions has been demonstrated by Searcy (1975) and Burke (1976). As the droplets penetrate through the altitude of minimum temperature to the lower boundary of the supersaturated region, they reach maximum size. Below this height, they evaporate by about a factor of 10 increasing rate for every 10°K increase in temperature

(Witt, 1969). Total evaporation will then occur near 80 km, explaining the sharp lower boundary observed for NLC. The water vapor freed by evaporation as well as incompletely evaporated particulates are available for recycling upward to replenish the supersaturation region. This is necessary to support continued NLC formation and also reduces the need for large external water and nucleation sources once the cycle is initiated.

Finally, we note that below the cloud region, the observed species are distributionally similar to the mid-latitude results. This further amplifies the unusual structure observed above 80 km, and the likelihood of its correlation with NLC characteristics.

SUMMARY AND CONCLUSIONS

We have presented ion mass spectrometer data obtained from two identical rocket-borne instruments, using nearly identical sampling techniques which permit subsonic sampling with low attractive bias potential in the prime region of interest. Comparison is made between the control data results (Wallops Island, Va.) and a high latitude sounding into apparent NLC conditions (Kiruna, Sweden).

In the mid-latitude (Wallops Island) results, all oxonium cluster ions through 91^+ are observed, with 73^+ and 55^+ being the most abundant species above and below 85 km, respectively. H_3O^+ (19^+) is conspicuous by its absence and is probably a dissociation product on flights where it is observed. Upleg ram and downleg

wake sampling are observed to produce identical results in the subsonic region of flight, verifying the suitability of this technique.

Above 80 km at Kiruna, the data are strikingly different from the Wallops Island results, and from all previously reported high latitude results. Within the NLC region, several groups of ions of 2 to 7 AMU width are observed to appear. Each of these groups contain one of the oxonium cluster ions 55^+, 73^+, 91^+, 109^+, or 127^+. By making identifications within the error limits of the measurement, it is possible to arrive at a consistent set of ions that relate exclusively to Fe^+, its oxides and its hydrates (Table 3). Evidence for the presence of excess H_2O is offered by the appearance of heavy water cluster ions of the oxonium group (91^+, 109^+, 127^+) and large quantities of 64^+ ($NO_2^+ \cdot H_2O$) and 66^+ ($NO^+ \cdot (H_2O)_2$) near 85 km. The unique composition structure of the above species appears consistent with current theories of NLC formation which require supersaturated water above a cold mesopause and a molecular or atomic nucleating agent such as Fe^+. The water is thought to be lifted by transport processes to cause the required supersaturation. Atomic and molecular ions then form complexes which may initiate growth of ice droplets. These droplets fall under gravitational attraction, reaching a maximum size underneath the mesopause, below which they are subject to rapid evaporation and recycling. The origin of the Fe^+ ions responsible for the observed cluster destributions is extraterrestrial, and is deposited in the 85 to 90 km domain by meteoric disintegration.

Since visibility of NLC's is extremely sensitive to particle size ($\sim 0.1\,\mu$ or larger), conditions for cloud formation are highly variable and intimately connected with nucleation processes. Excessive quantities of condensation nuclei may in fact retard or prevent NLC formation by exhaustion of the limited water supply. Because the presence of NLC's at the time of launch was not established, the ion composition observed could instead represent structure present during the formation or disappearing stages for an NLC.

The data below 80 km are quite similar for the two measurements, further amplifying the uniqueness of the results for the NLC domain.

The results presented here are self consistent, but require additional theoretical and experimental verification to establish reproducibility and uniqueness. Future measurements of this type should include simultaneous rocket-borne photometric studies to establish the exact cloud height and thickness, as well as temperature soundings to determine the precise magnitude and location of the mesopause.

ACKNOWLEDGEMENTS

This research occurred through a cooperative scientific program between members of the Swedish Board for Space Activities and the National Aeronautics and Space Administration. The results were successfully obtained with the competent efforts of the Chemosphere Branch (GSFC). In particular, we are indebted to Dr. A. C. Aikin for essential contributions during the planning and

implementation of this program. We thank Messrs. Giles Spaid, Donald Silbert, J. Roy Hagemeyer and R. Denis Endres for the development and preparation of the flight payloads. We also thank Mr. Nathan Wilhelm of the University of Stockholm for providing airborne observations of NLC during the campaign period. We also acknowledge the extensive technical support provided by the Wallops Flight Center and the Swedish Space Corporation, which made this cooperative effort possible. One of us (G. W.) was supported by the Swedish Board for Space Activities under contract number DR 317.

REFERENCES

Aikin, A. C., R. A. Goldberg, Y. V. Somayajulu and M. B. Avadhanulu: Electron and Positive Ion Density Altitude Distributions in the Equatorial D-Region, J. Atmos. Terrestrial Phys., 34, 1483-1494, 1972

Aikin, A. C., J. A. Kane and J. Trim: Some Results of Rocket Experiments in the Quiet D Region, J. Geophys. Res., 69, 4621-4628, 1964

Burke, R. R.: Mechanism for Noctilucent Cloud Foundation, presented at COSPAR, Philadelphia, Pennsylvania, 1976

Castleman, A. W., Jr.: Nucleation Processes and Aerosol Chemistry, Space Sci. Rev., 15, 547-589, 1974

Castleman, A. W., Jr.: Relationship Between Ions, Nucleation, and Aerosol Formation, EOS Trans. AGU, 57, 302, 1976

Chapman, S. and P. C. Kendall: Noctilucent Clouds and Thermospheric Dust: Their Diffusion and Height Distribution, Quart. J. Roy. Met. Soc., 91, 115-131, 1965

Christie, A. D.: A Condensation Model of Noctilucent Cloud Formation, Space Res., 9, 175-182, 1969a

Christie, A. D.: The Genesis and Distribution of Noctilucent Cloud, J. Atmos. Sci., 26, 168-176, 1969b

Donahue, T. M., B. Guenther and J. E. Blamont: Noctilucent Clouds in Daytime: Circumpolar Particulate Layers Near the Summer Mesopause, J. Atmos. Sci., 29, 1205-1209, 1972

Fiocco, G. and G. Grams: On the Origin of Noctilucent Clouds: Extraterrestrial Dust and Trapped Water Molecules, J. Atmos. Terrestrial Phys., 33, 815-824, 1971

Gadsden, M.: Observation of the Color and Polarization of Noctilucent Clouds, Ann. Geophys., 31, 507-516, 1975

Goldberg, R. A. and A. C. Aikin: Studies of Positive Ion Composition in the Equatorial D-Region Ionosphere, J. Geophys. Res., 76, 8352-8364, 1971

Goldberg, R. A. and A. C. Aikin: Subsonic Sampling of Positive Ion Composition in the Ionospheric D-Region, EOS Trans. AGU, 53, 1077, 1972

Goldberg, R. A. and L. J. Blumle: Positive Ion Composition from a Rocket-Borne Mass Spectrometer, J. Geophys. Res., 73, 133-142, 1970

Grishin, N. I.: Wave Motion and Meteorlogical Conditions for the Appearance of Noctilucent Clouds, Ann. Int. Geophys. Yr., 11, 20-22, 1961

Hemmenway, C. L., R. K. Soberman and G. Witt: Investigations of Noctilucent Cloud Particles, Tellus, 16, 84-109, 1964

Hesstvedt, E.: Nucleation and Growth of Noctilucent Cloud Particles, Space Res., 9, 170-174, 1969

Hummel, J. R. and J. J. Olivero: Satellite Observation of the Mesospheric Scattering Layer and Implied Climatic Consequences, J. Geophys. Res., 81, 1976 (In Press)

Jesse, O. Die Höhe der leuchtenden Nachtwolken, Astr. Nachr., 140, 161-168, 1896

Johannessen, A. and D. Krankowsky: Positive Ion Composition Measurement in the Upper Mesosphere and Lower Thermosphere at a High Latitude During Summer, J. Geophys. Res., 77, 2888-2901, 1972

Johannessen, A., D. Krankowsky, F. Arnold, W. Riedler, M. Friedrich, K. Folkestad, G. Skovli, E. V. Thrane, J. Tröim: Detection of Water Cluster Ions at the High Latitude Summer Mesopause, Nature, 235, 215-217, 1972

Millman, P. M. and D. W. R. McKinley: Meteors, in The Moon, Meteorites, and Comets, ed by B. M. Middlehurst and G. P. Kuiper, U. of Chicago Press, Chicago, Ill., USA, 1963

Narcisi, R. S. and A. D. Bailey: Mass Spectrometric Measurements of Positive Ions at Altitudes from 64 to 112 Kilometers, J. Geophys. Res., 70, 3687, 1965

Narcisi, R. S. and W. Roth: The Formation of Cluster Ions in Laboratory Sources and in the Ionosphere, Advan. Electron. Electron Phys., 29, 79, 1970

Proceedings of International Symposium on Noctilucent Clouds (Tallin, 1966) ed by I. A. Khvostikov and G. Witt, Moscow 1967

Rauser, P. and H. Fechtig: Combined Dust Collection and Detection Experiment During a Noctilucent Cloud Display above Kiruna, Sweden, Space Res., 12, 391-402, 1972

Reid, G. C.: Ice Clouds in the Summer Polar Mesopause, J. Atmos. Sci., 32, 523-535, 1975

Searcy, J. Q.: A Kinetic Model for Clustering of Water on Hydrated Protons in a Supersonic Free Jet Expansion, J. Chem. Phys., 63, 4114-4119, 1975

Soberman, R. K.: Extraterrestrial Origin of Noctilucent Clouds, Space Res., 9, 183-189, 1969

Störmer, C.: Height and Velocity of Luminous Night Clouds Observed in Norway; 1932 — Oslo University Obs. Publs. #6, 1933

Theon, J. S., W. Nordberg, L. B. Katchen and J. J. Horvath: Some Observations on the Thermal Behavior of the Mesosphere, J. Atmos. Sci., 24, 428-438, 1967

Tozer, W. F. and D. E. Beeson: Optical Model of Noctilucent Clouds Based On Polarimetric Measurements From Two Sounding Rocket Campaigns, J. Geophys. Res., 79, 5607-5612, 1974

Witt, G.: Height Structure and Displacements of Noctilucent Clouds, Tellus, 14, 1-18, 1962

Witt, G.: Optical Characteristics of Mesopheric Aerosol Distributions in Relation to Noctilucent Clouds, Tellus, 20, 98-113, 1967

Witt, G.: The Nature of Noctilucent Clouds, Space Res., 9, 157-169, 1969

Witt, G., J. Stegman and H. Wood: High-Latitude Noctilucent Cloud and Sodium Layers near the Mesopause, in Methods of Measurements and Results of Lower Ionospheric Structure, ed by K. Rawer, p. 431-445, Akademie-Verlag, Berlin, 1974

Zbinden, P. A., M. A. Hidalgo, P. Eberhardt, and J. Geiss: Mass Spectrometer Measurements of the Positive Ion Composition in the D- and E-Regions of the Ionosphere, Planet. Space Sci., 23, 1621-1642, 1975

Table 1

Flight and Launch Range Specifications

Parameter	NASA 10.412	NASA 10.414
Date 1973	June 30	August 2
Launch Time (LMT)	1510	0700
Solar Zenith Angle	43.0°	68.5°
Payload Weight (kg)	68.9	70.1
Diameter (cm)	22.9	22.9
Spin Rate (Hz)	4.3	4.8
Coning Angle	±4.5°	<±2°
Coning Period (sec)	2.4	2.1
Trajectory Azimuth (clockwise from North)	133°	354°
Payload aspect		
Azimuth	117°	030°
Elevation	76°	81°
Apogee Altitude (km)	86.5	90.0
Range Location	Wallops Island	Kiruna
Latitude	37.8 N	67.9° N
Longitude	75.5 W	21.1° E
Magnetic Dip	68.8°	76.7°

Table 2

Spectrometer Characteristics

Characteristic	10.412	10.414
Entrance Aperture Diameter (mm)	.742	.742
Rod Length (cm)	15.2	15.2
Sampling Interval (sec)	5.75	6.03
Approximate Sweep Range, AMU	15→143	12→148
Time/Unit Mass (sec)	.0423	.0417
RF (MHz)	2.037	2.037
Attractive Bias Potential (volts)	-5.4	-5.6

Table 3

Suggested Identifications For The Cluster Ion Groups A → E

Identified Within The NLC Region Aboard NASA 10.414

GROUP					
A			55^+ $H_3O^+ \cdot (H_2O)_2$	56^+ Fe^+	
B		72^+ FeO^+	73^+ $H_3O^+ \cdot (H_2O)_3$ $FeOH^+$	74^+ $Fe^+ \cdot H_2O$	
C	88^+ FeO_2^+	90^+ $FeO^+ \cdot H_2O$	91^+ $H_3O^+ \cdot (H_2O)_4$	92^+ $Fe^+ \cdot (H_2O)_2$	
D	106^+ $FeO_2^+ \cdot H_2O$	108^+ $FeO^+ \cdot (H_2O)_2$	109^+ $H_3O^+ \cdot (H_2O)_5$	110^+ $Fe^+ \cdot (H_2O)_3$	112^+ Fe_2^+ ?
E	124^+ $FeO_2^+ \cdot (H_2O)_2$	126^+ $FeO^+ \cdot (H_2O)_3$	127^+ $H_3O^+ \cdot (H_2O)_6$	128^+ $Fe^+ \cdot (H_2O)_4$ Fe_2O^+	

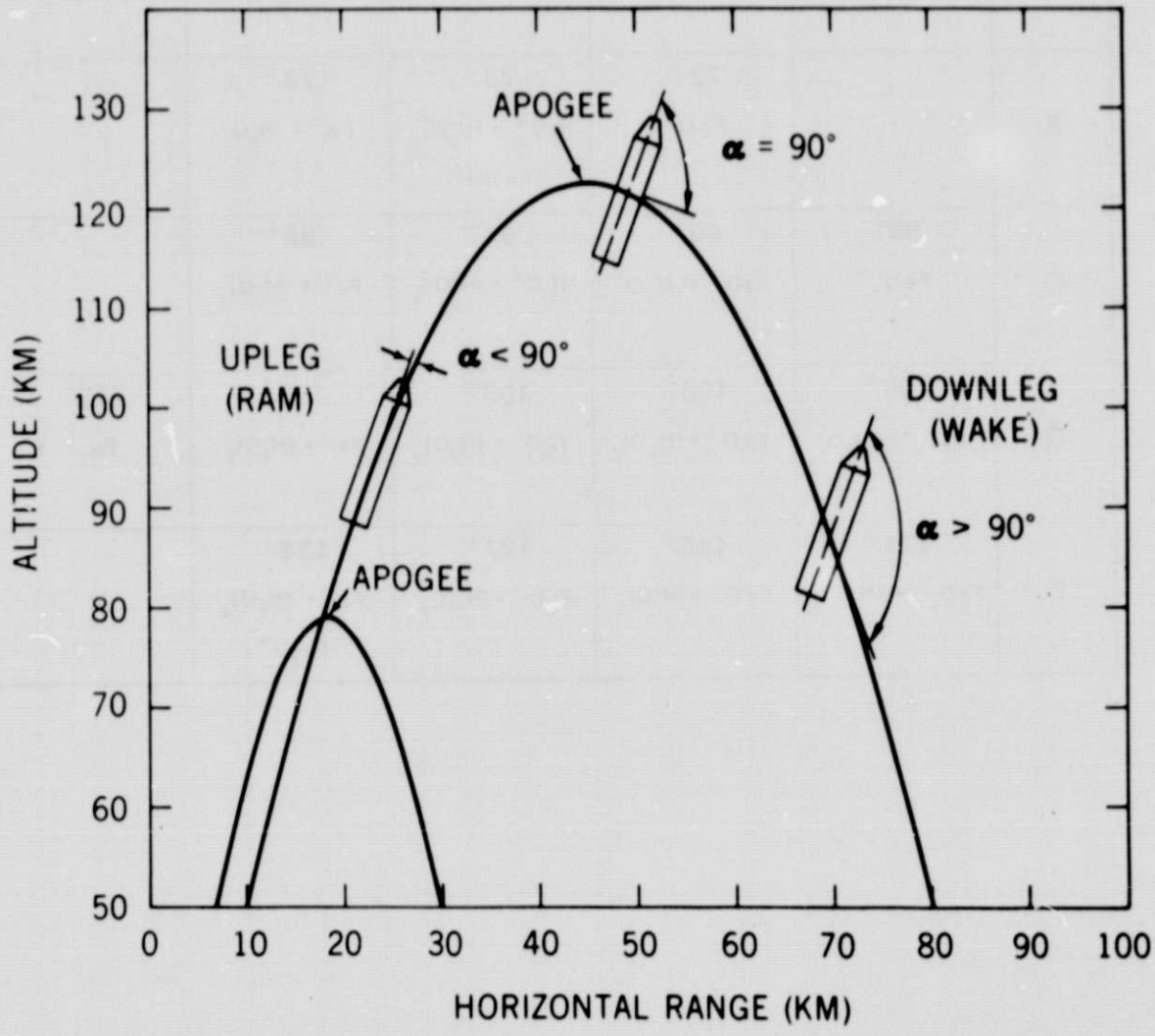

Figure 1. Comparison of low and high altitude trajectories for mesospheric sampling. Conditions of ram and wake sampling are depicted by $\alpha < 90^\circ$ or $\alpha > 90^\circ$, respectively.

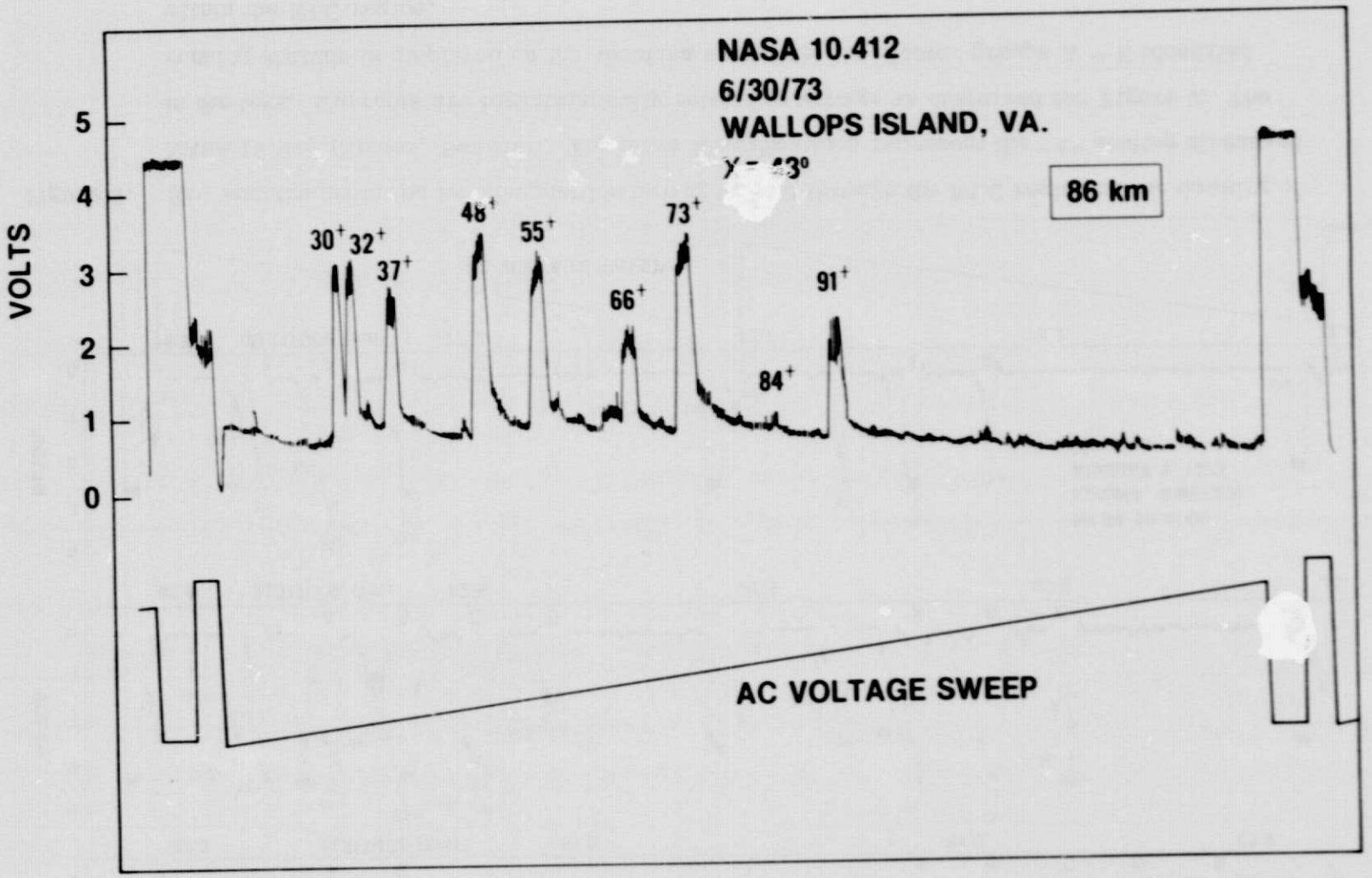

Figure 2. Sample raw ion mass spectrum obtained near apogee for NASA 10.412 at Wallops Island, Va. The voltage display is nearly logarithmic in current and therefore in relative composition among species. The linear AC voltage sweep is also displayed.

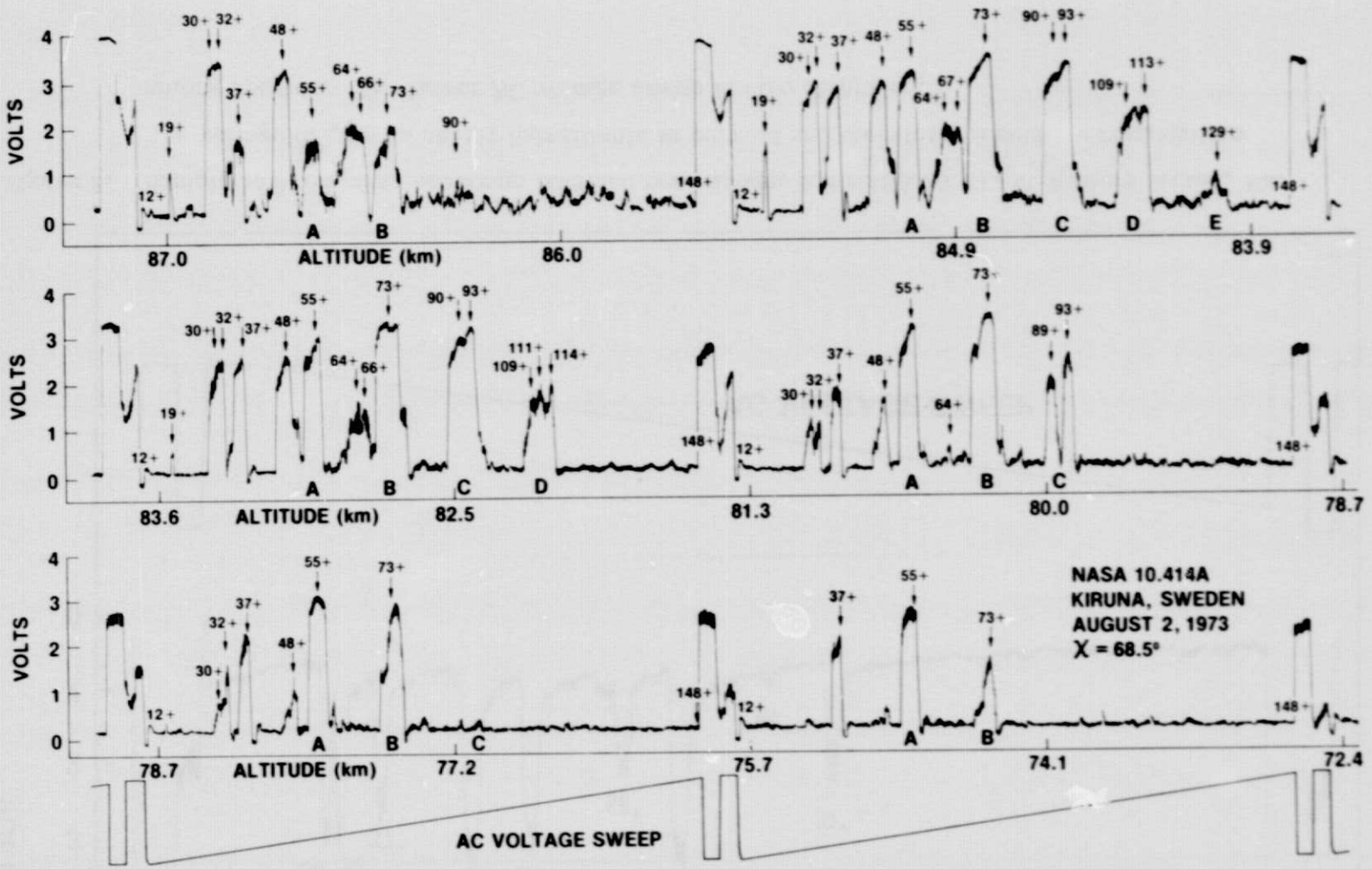

Figure 3. Raw spectra depicting ion composition during transit through the NLC region on the downleg of NASA 10.414 (Kiruna, Sweden). The mass identifications represent the "A" scaling discussed in the text. Currents are logarithmically related to voltage as discussed for Figure 2. The running altitude is displayed on the abscissa along with the cluster groups A → E identified within the NLC region.

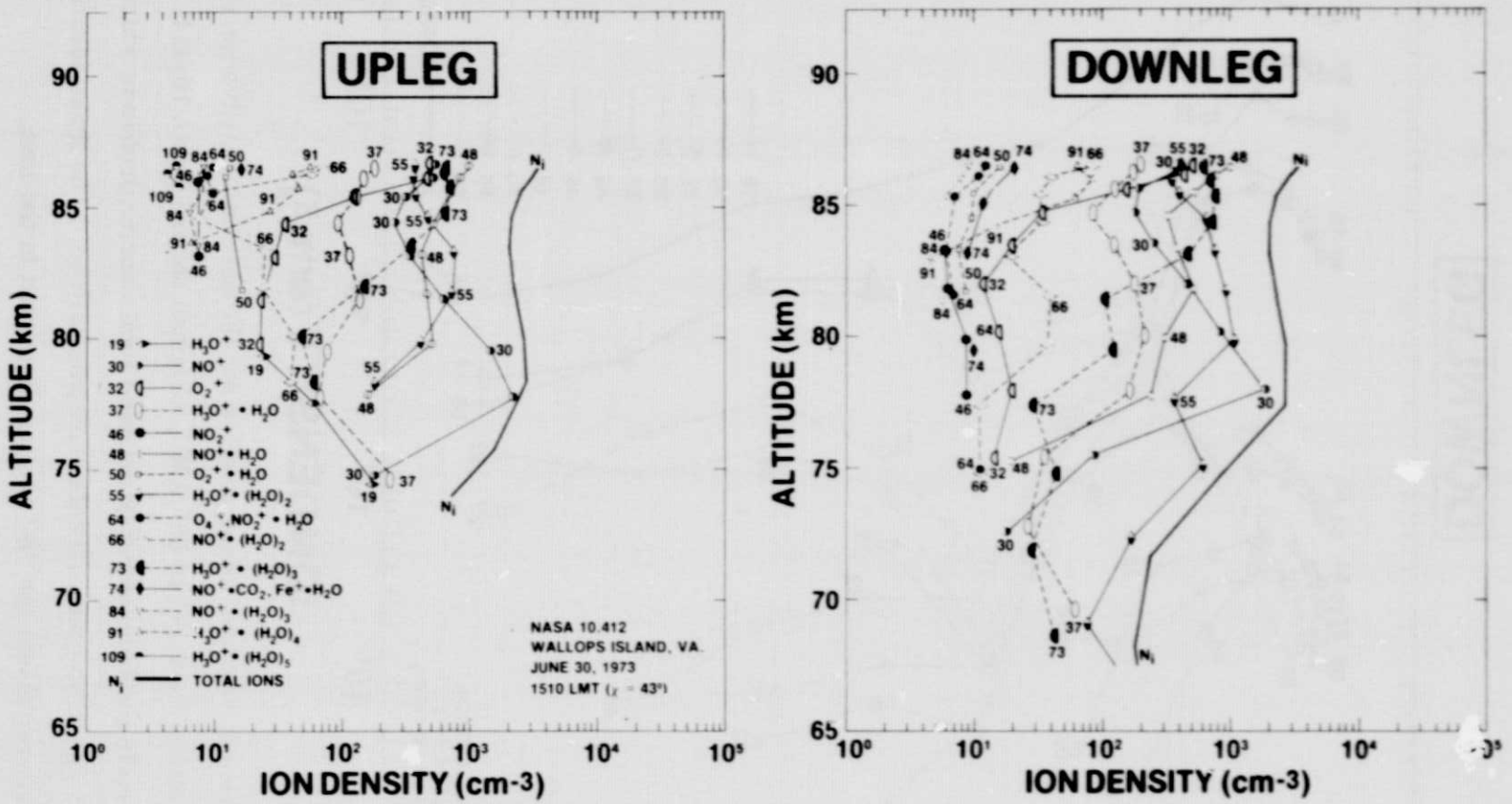

Figure 4. Comparison between upleg and downleg vertical height profiles for the absolute positive ion composition obtained aboard NASA 10.412 at Wallops Island, Va. N_i depicts the total density profile to which the ion spectrometer results were normalized. Probable identifications for each mass number are listed in the key.

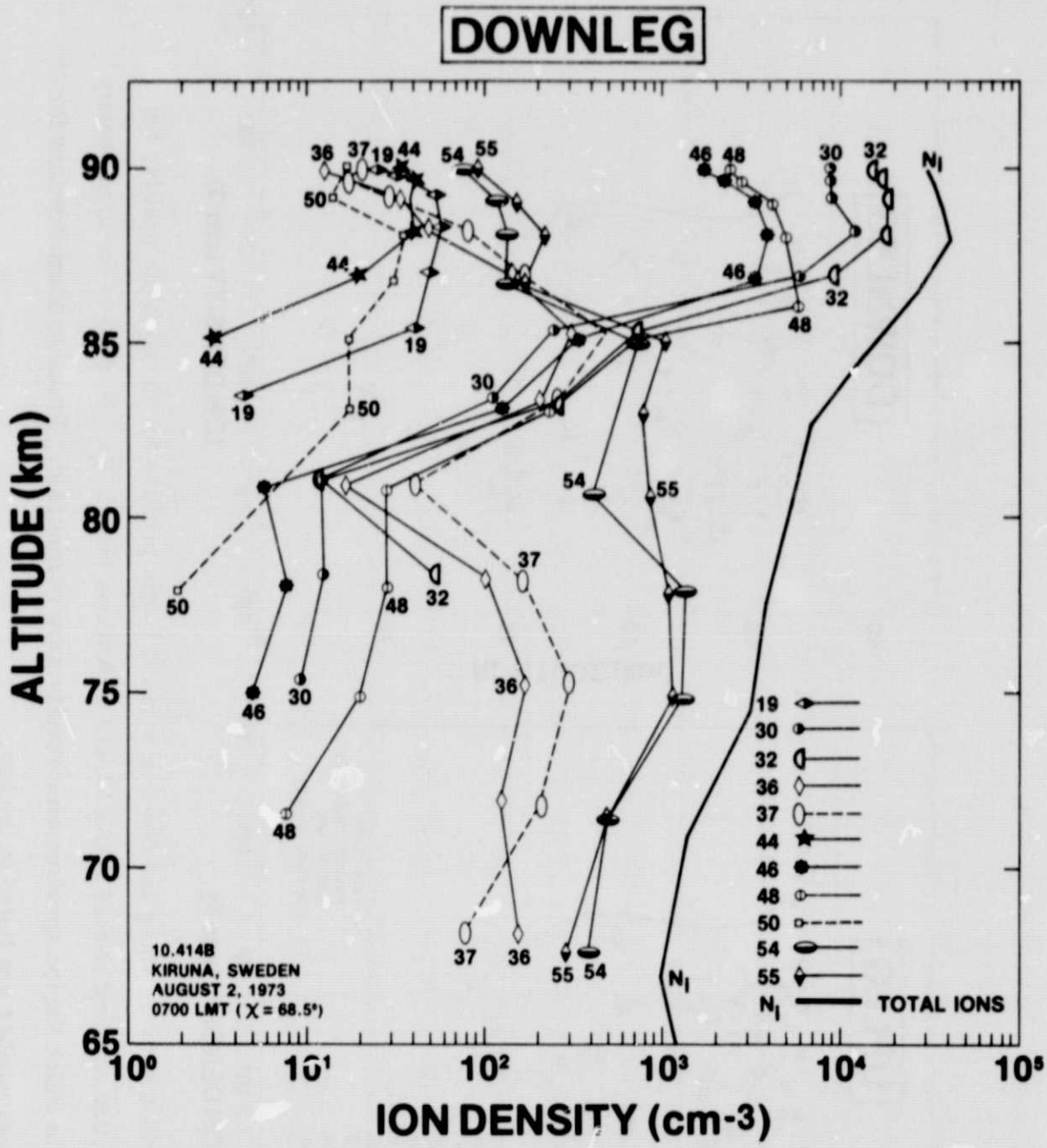

Figure 5. Downleg vertical height profiles for the absolute positive ion composition from 19^+ to 55^+ AMU, obtained aboard NASA 10.414. N_i depicts the independently obtained total density profile to which the ion spectrometer currents were normalized. The mass identifications represent the "B" scaling discussed in the text.

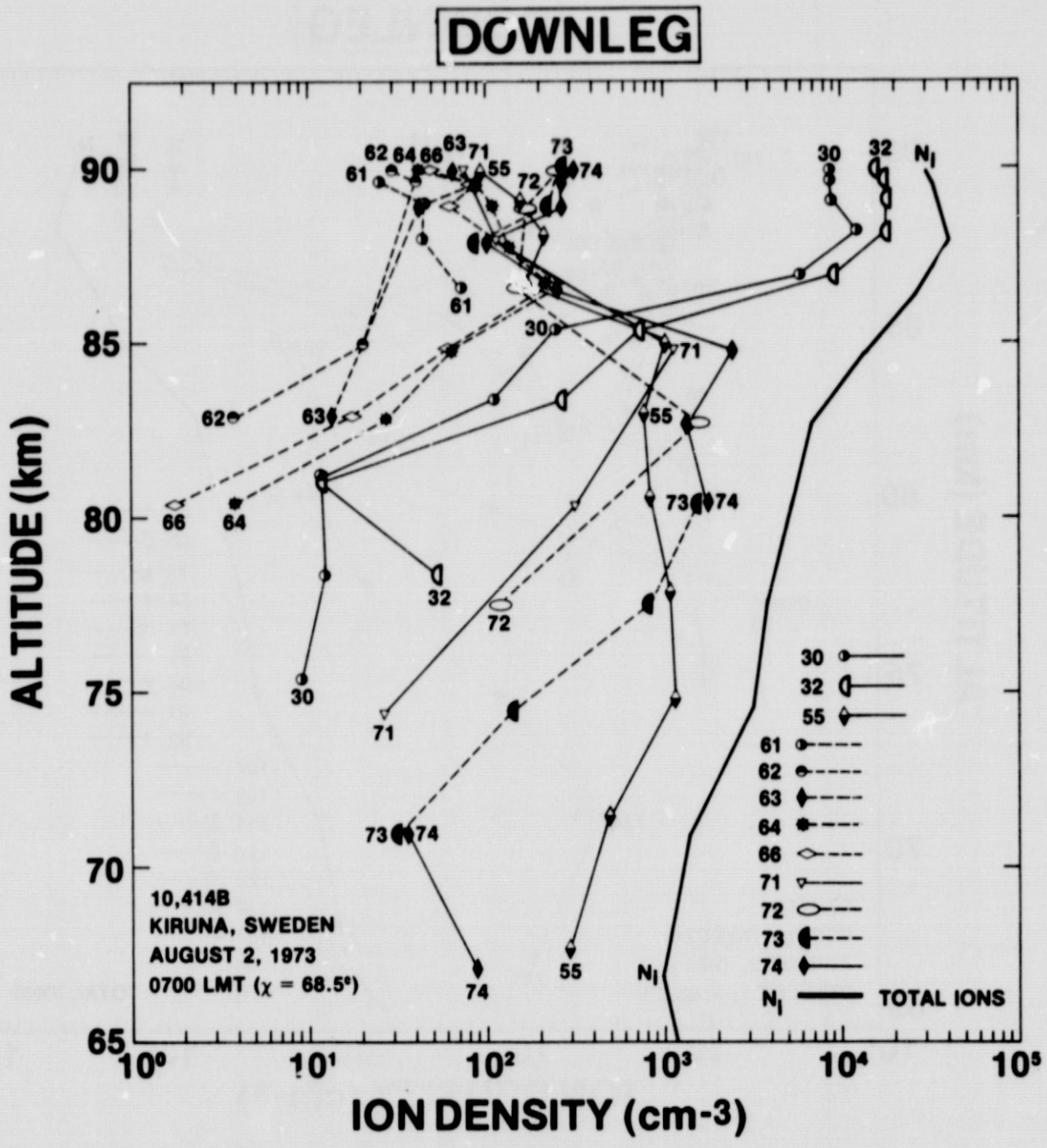

Figure 6. Downleg vertical height profiles for the absolute positive ion composition from 55^+ to 74^+ AMU, obtained aboard NASA 10.414. N_i, 30^+ and 32^+ are repeated from Figure 5 for comparison. The mass identifications represent the "B" scaling discussed in the text.

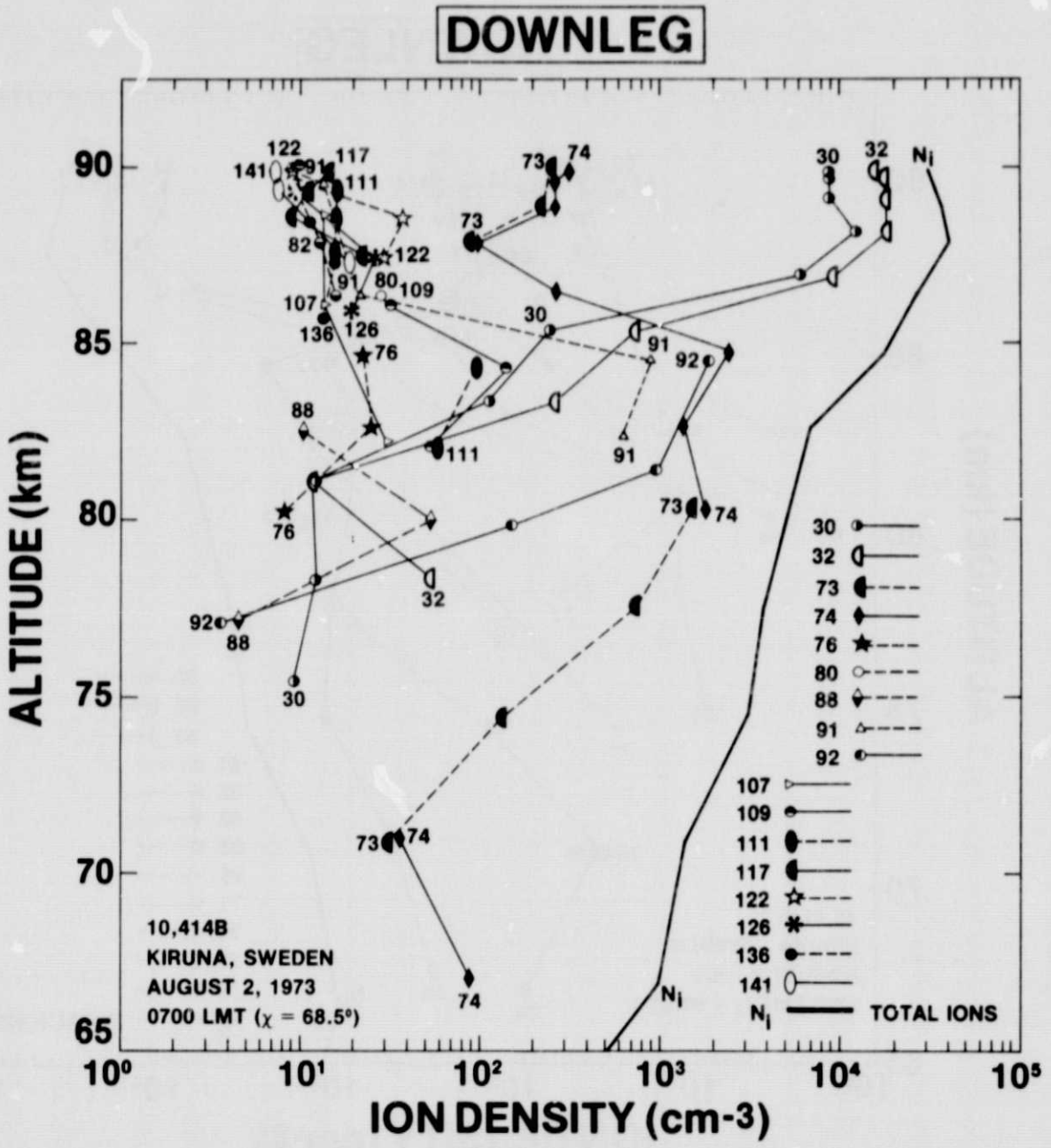

Figure 7. Downleg vertical height profiles for the absolute positive ion composition from 73^+ to 141^+ AMU, obtained aboard NASA 10.414. N_i, 30^+ and 32^+ are repeated for comparison. The mass identifications represent the "B" scaling discussed in the text.

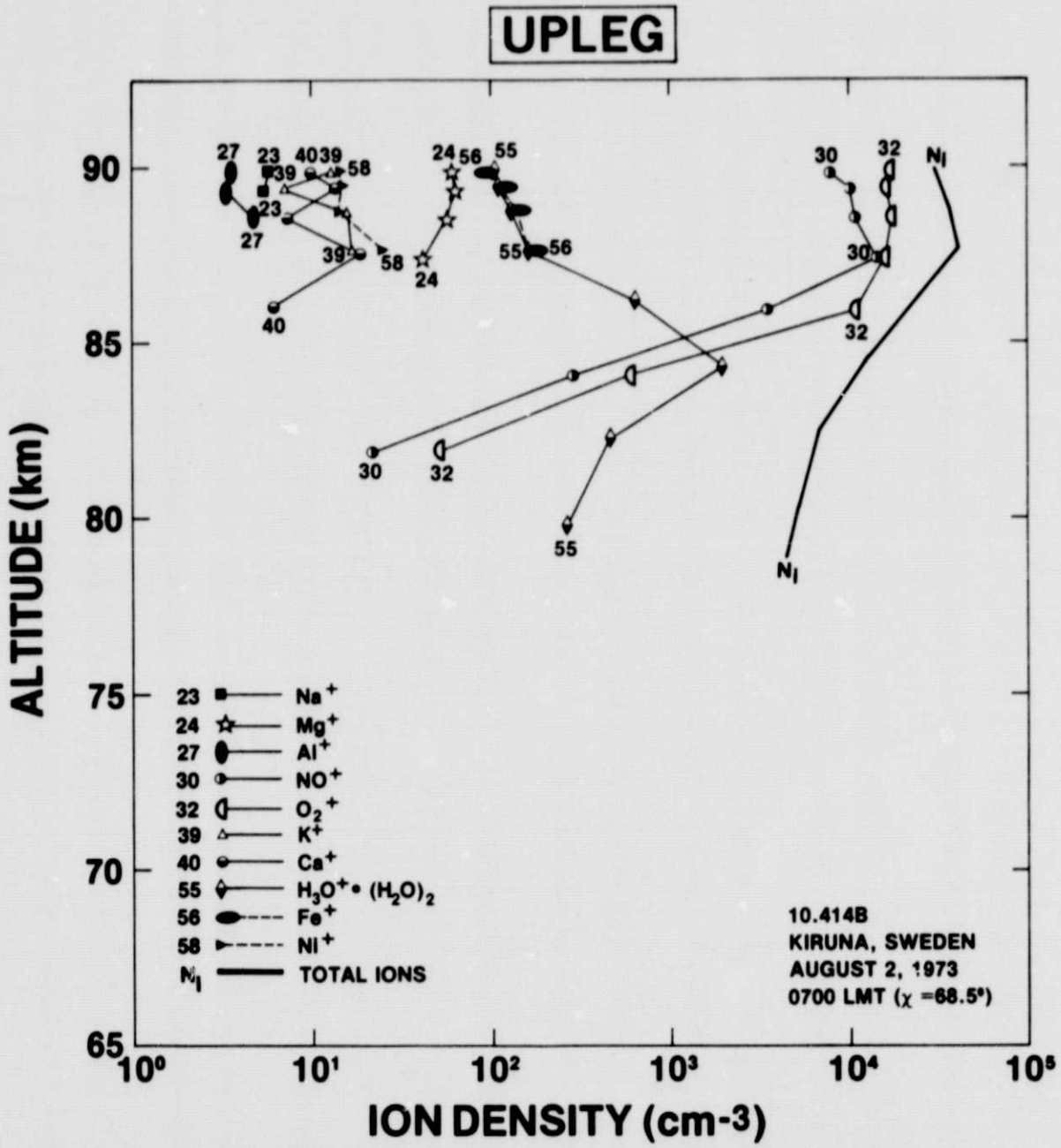

Figure 8. Upleg vertical profiles for the metallic ion species observed aboard NASA 10.414. N_i, 30^+, 32^+ and 55^+ are also illustrated for comparison.